HIGH ENERGY COSMIC RAY CHARGE AND ENERGY SPECTRA MEASUREMENTS

J.H. Chappell and W.R. Webber

Space Science Center
University of New Hampshire
Durham, N.H. 03824
U. S. A.

In 1976, 1977, and 1978, we have conducted a series of 3 balloon flights to measure the energy spectra of cosmic ray nuclei. A gas Cerenkov detector with different gas thresholds of 8.97, 13.12, and 17.94 GeV/nuc was employed to extend these measurements to high energies. The total collection factor for these flights is > 20m^2 ster-hr. Individual charge resolution is achieved over the charge range Z=4-26, and overlapping differential spectra are obtained from the 3 flights up to $\sim$ 100.0 GeV/nuc.

Instrument. A schematic diagram of the instrument used for the three flights is shown in Figure 1. The key element for the high energy measurement is a 25.0 cm thick Freon-12 filled gas Cerenkov detector. Absolute gas pressures were selected to give energy thresholds of 8.97, 13.12, and 17.94 GeV/nuc respectively. The Cerenkov photons in this counter were collected by two separate banks of four 5 in. diameter photomultiplier tubes. A total of 6.3, 3.4, and 1.7 photoelectrons were observed for β=1, Z=1 particles for the three gas pressures respectively. A multielement array of solid Cerenkov and scintillator counters was used to determine the charge and the radial entry point of the cosmic rays in the telescope.

Data Analysis. A set of consistency criteria were applied to the two scintillators and the solid Cerenkov detectors to remove interacting events in the telescope. The charge was determined by crossplots of (S+C)/2 versus the average pulse height from the gas Cerenkov detector. Figure 2 shows the charge resolution for the 1976 flight for events >10.0 GeV/nuc. The total amount of material in the telescope was 8.71, 10.0, and 4.71 gm/cm^2 respectively. Atmospheric corrections were performed using an atmospheric slab model of 4.03, 3.50, and 4.51 gm/cm^2 respectively. A more detailed description of the flight and data analysis will be published at a later date.

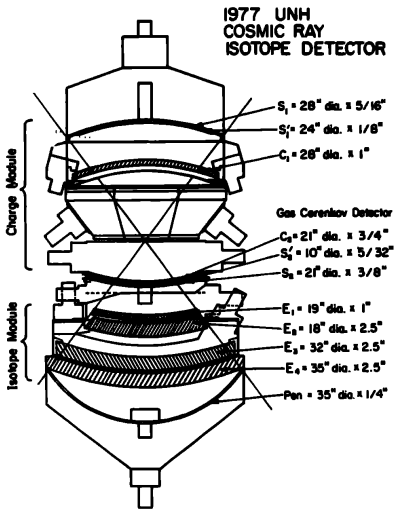

Figure 1. Schematic diagram of the 1977 instrument. The 1976 and 1978 were similar in design.

	1976		1977		1978	
	RC	CRC	RC	CRC	RC	CRC
	E_k>9.72 GeV		E_k>16.15 GeV		E_k>25.30 GeV	
B	174	281	161	216	115	197
C	958	1741	1165	2216	706	1401
N	184	326	230	418	106	197
O	983	1884	1290	2256	700	1454
F	18	36	24	46	16	31
Ne	130	253	198	403	94	197
Na	21	41	30	61	17	34
Mg	187	413	215	484	115	256
Al	34	70	37	68	20	38
Si	157	354	156	357	90	204
P	-	-	-	-	-	-
S	30	73	25	60	15	36
Cl	9	19	8	19	6	12
Ar	1	25	10	25	6	13
K	6	14	9	21	6	13
Ca	17	44	15	38	10	23
Sc	5	6	4	9	2	4
Ti	7	17	9	21	2	4
V	7	17	11	26	2	4
Cr	11	21	9	23	6	16
Fe	88	273	104	320	65	185

Table 1. Shows the raw counts (RC) and the total number of events corrected to the top of the atmosphere (CRC) for each flight above the usable Cerenkov threshold.

The measurements presented in this paper represent improvements over previous measurements in two areas. 1) These measurements have the greatest statistical accuracy over a large energy range and high energy charge resolution of any measurements made to date. 2) By demanding a consistency between the three flights, we believe that we have been successful in eliminating systematic errors in the derivation of the spectra.

The differential spectra were derived by the deconvolution techniques described by Lezniak (1975). At energies above the last energy bin of .95 G/G_m the integral flux was converted to a differential flux by the relationship

$$j(E) = \frac{(\gamma-1)\ J\ (E \rightarrow \infty)}{E}$$

For the abundant nuclei, individual differential and integral intensities have been calculated. The less abundant charges have been combined into groups and their associated intensities determined. Table 1 lists the total number of raw counts and corrected raw counts above the usable Cerenkov threshold for the three flights. Figure 3 shows the differential flux times $E^{2.5}$ vs. energy for selected nuclei.

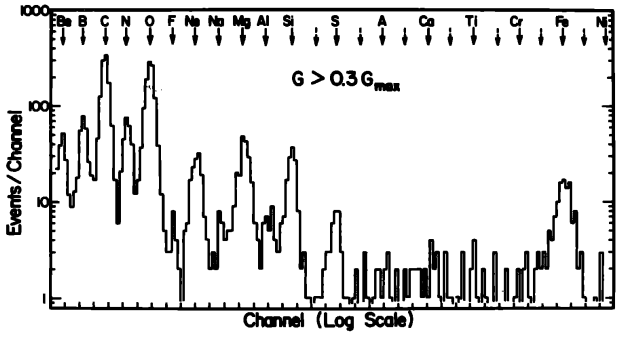

Figure 2. Charge histogram for the 1976 flight for kinetic energies above ~ 9.72 GeV/nuc.

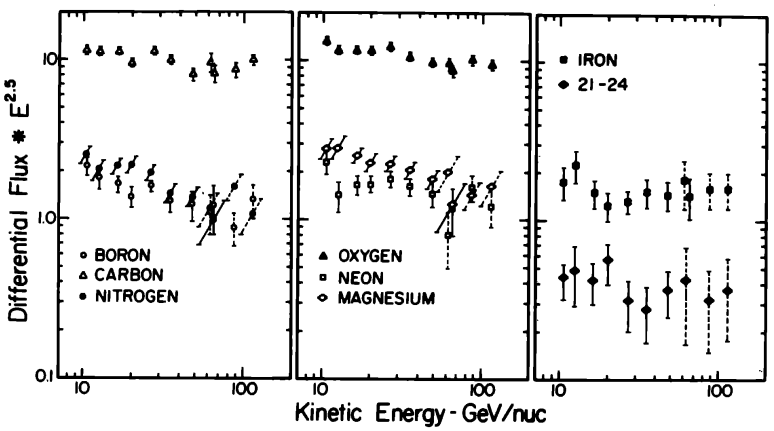

Figure 3. Differential flux $*E^{2.5}$ versus kinetic energy for the combined data set.

Discussion and Conclusions. By inspecting the differential spectras of the primary species, one finds that there are two general features. 1) The spectral index of the nuclei is slowly changing as a function of energy. The spectrum is steepening at the higher energies. For example, carbon and oxygen between the energy ranges of 10 to 30 GeV/nuc have spectral indices of -2.53 and -2.63 respectively. In the interval between 30.0 and 100.0 GeV/nuc, the spectra steepen to -2.63 and -2.65. 2) There is a trend for the lower Z primary nuclei to have an overall steeper slope than the higher Z primary elements. Carbon, oxygen and iron have a overall best fit spectral index of -2.65, -2.65 and -2.53 respectively. The low Z nuclei have spectral indices which are close to the observed proton spectrum.

In the context of a diffusive or leaky box model, these features can be explained by the competing effects of the galactic escape and nuclear interactions, assuming that the injection spectra of these nuclei are similar and have constant exponents above $\sim$ 10 GeV/nuc.

The spectra of the secondary nuclei are in general steeper than that of their respective primaries. These nuclei are produced mainly by spallation of the primaries. The observed steepening of the spectrum can be attributed to the energy dependence of the escape mean free path and the consequent passage of the primaries through less interstellar matter.

The secondary to primary ratios are of prime interest in determining the path length distribution and the escape parameters. Several ratios have been plotted in Figure 4. The low energy data points spanning the energy range from 0.95 to 6.0 GeV/nuc are those reported from Lezniak and Webber,1978. The general observations of the data indicate that all of the ratios decrease as a function of energy. The ratios imply that the primaries have traversed a path length of $\sim$ 7 g/cm^2 at 1 GeV/nuc which steadily decreases to about $\sim$1 g/cm^2 at 100 GeV/nuc. In the propagation calculations we have assumed that B and Z=21-24 have a zero source component. The other charges that have a non-zero source component were based on source ratios of $(17\text{-}19)_s = .035\ Fe_s$, $(9+11+13)_s = .047\ (10+12+14)_s$, and $N_s = .05\ O_s$. It should be noted that all of the ratios measured are in remarkably close agreement. The B/C and Z=21-24/Fe ratios have been plotted versus their apparent exponential escape length in Figure 5. Using

the combined data set, the average escape mean free path is

$$\langle\lambda_e\rangle = (7.21\pm.86)E^{-(0.32\pm0.10)}$$

over the energy range 1-100 GeV/nuc.

Although the statistics are limited, the data shows a possible flattening of the escape mean free path at energies >50.0 GeV/nuc. If this feature is correct, it would indicate a break in the energy dependent path length, a feature with considerable significance for the propagation and/or acceleration of the primary radiation.

The authors are appreciative of NASA Grant NGR-30-002-052 for support of this research.

References

Lezniak, J.A., 1975, Nucl. Instr. Meth. 126, 129.
Lezniak, J.A., and Webber, W.R., 1978, Astrophysical Journal, 223, 676.

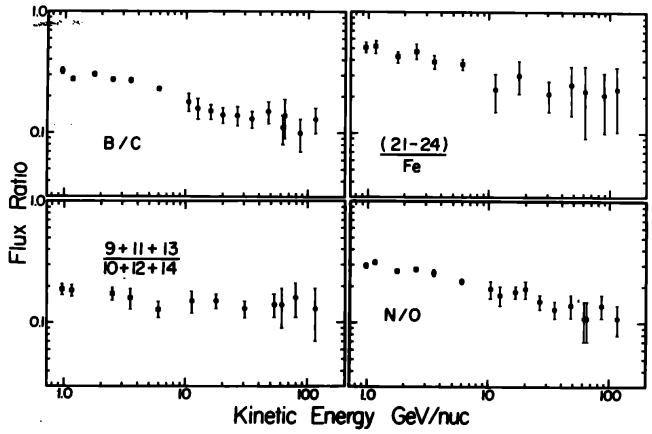

Figure 4. Secondary to primary charge ratios vs. kinetic energy.

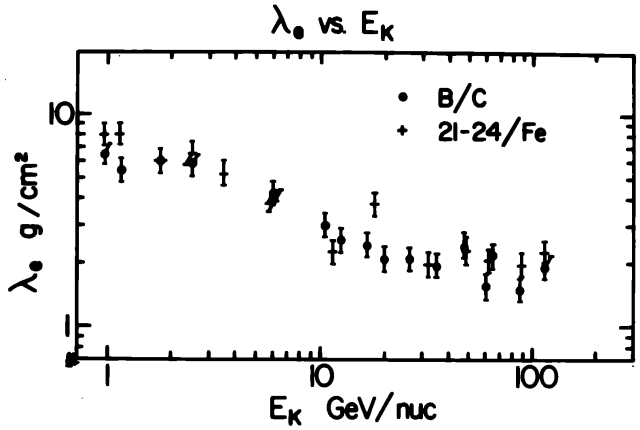

Figure 5. Apparent escape mean free path versus kinetic energy.